Supplementary Material

Optical scatter imaging of resected breast tumor structures matches the patterns of micro-computed tomography

Samuel S. Streeter[1], Benjamin W. Maloney[1], Rebecca A. Zuurbier[2,3], Wendy A. Wells[2,3], Richard J. Barth[2,3], Keith D. Paulsen[1,3], and Brian W. Pogue[1,3]

[1] Thayer School of Engineering, Dartmouth College, Hanover, NH 03755, United States of America
[2] Departments of Radiology (RAZ), Pathology and Laboratory Medicine (WAW), and Surgery (RJB), Dartmouth-Hitchcock Medical Center, Lebanon NH 03756, United States of America
[3] Norris Cotton Cancer Center, Dartmouth-Hitchcock Medical Center, Lebanon NH 03756, United States of America

Email: Samuel.S.Streeter.TH@Dartmouth.edu and Brian.W.Pogue@Dartmouth.edu

Appendix 1: Imaging System

Multimodal imaging system specifications and schematics are published elsewhere (McClatchy *et al* 2017). The optical imaging method used in this study is referred to as spatial frequency domain imaging (SFDI). SFDI involves projecting one-dimensional sinusoidal patterns of light onto biological tissue in a reflectance geometry. The same spatial frequency pattern is imaged three times with pattern phase shifts of Φ=0°, 120°, and 240°. Three-phase, pixel-by-pixel amplitude demodulation combines monochromatic phase images into a reflectance map corresponding to a single spatial frequency and optical wavelength (Cuccia *et al* 2005). By imaging at multiple spatial frequencies, the modulation transfer function of the sample can be discretely measured. The experimental modulation transfer function is typically fit to an appropriate diffuse or sub-diffuse light transport model to approximate pixel-level optical properties (i.e., absorption coefficient, reduced scattering coefficient, and/or a phase function parameter) of the sample (Cuccia *et al* 2009, Kanick *et al* 2014). Optical property quantification in the diffuse light transport regime is the most common application of SFDI. At the highest spatial frequencies of illumination, however, the measured reflectance is dominated by sub-diffusely scattered photons, which

undergo few scattering events followed by singular, large backscattering events to the detector. Under these circumstances, the imaging method is called sub-diffuse SFDI (sd-SFDI). Sd-SFDI reflectance contrast is dominated by optical scatter, because the impact of absorption is greatly diminished (Krishnaswamy *et al* 2014). Additionally, short optical wavelengths exhibit higher sensitivity to scattering relative to longer wavelengths (Jacques 2013). Thus, for the purposes of this study, "optical scatter imaging" is sd-SFDI only at the highest spatial frequency (f_x = 1.37 mm^{-1}) and shortest optical wavelength (λ = 490 nm) possible to maximize contrast to light backscattering (these f_x and λ values were limited by the digital light projector and laser source, respectively, in the multimodal imaging system used in this study). See Multimedia S1 for a video demonstration of monochromatic (λ = 490 nm), multi-spatial frequency SFDI acquisition from two representative specimens in the dataset.

Appendix 2: Image Data

Supplementary Figure S1 demonstrates the co-registration of histologic images to wide field-of-view optical and micro-CT imagery. Micro-CT slices and optical images for some specimens contain small, interior patches of black pixels. These pixels correspond to regions of tissue that were not in contact with the top acrylic plate during imaging and were thus irregular in surface profile. Irregular tissue surfaces are prone to specular reflection artifacts in the optical images. To mitigate specular reflection artifacts, non-tissue pixels in the micro-CT slice were used as a mask for the co-registered optical images to remove interior air gaps and tissue edges from the analysis.

Appendix 3: Image Analysis

Supplementary Figure S2 provides an overview of the image similarity analysis performed in this study. The similarity metrics used were mutual information (MI) and the Sørensen–Dice coefficient (Dice), and the quantification of each of these metrics is illustrated in Supplementary Figures S3 and S4, respectively. MI was quantified using four-bit (1-16 integer intensity levels) scaled versions of the images. Supplementary Figure S5 illustrates the quantification of the coefficient of variation.

Supplementary Material References

Cuccia D J, Bevilacqua F, Durkin A J, Ayers F R and Tromberg B J 2009 Quantitation and mapping of tissue optical properties using modulated imaging. *J. Biomed. Opt.* **14** 024012

Cuccia D J, Bevilacqua F, Durkin A J and Tromberg B J 2005 Modulated imaging: quantitative analysis and tomography of turbid media in the spatial-frequency domain. *Opt. Lett.* **30** 1354–6

Jacques S L 2013 Optical properties of biological tissues: a review. *Phys. Med. Biol.* **58** R37-61

Kanick S C, McClatchy D M 3rd, Krishnaswamy V, Elliott J T, Paulsen K D and Pogue B W 2014 Sub-diffusive scattering parameter maps recovered using wide-field high-frequency structured light imaging. *Biomed. Opt. Express* **5** 3376–90

Krishnaswamy V, Elliott J T, McClatchy D M 3rd, Barth R J J, Wells W A, Pogue B W and Paulsen K D 2014 Structured light scatteroscopy. *J. Biomed. Opt.* **19** 070504

McClatchy D M, Rizzo E J, Meganck J, Kempner J, Vicory J, Wells W A, Paulsen K D and Pogue B W 2017 Calibration and analysis of a multimodal micro-CT and structured light imaging system for the evaluation of excised breast tissue. *Phys. Med. Biol.* **62** 8983–9000

Supplementary Material Multimedia and Figure Captions

(See separate MP4 video file.)

Multimedia S1. Monochromatic (λ = 490 nm), multi-spatial frequency (f_x) SFDI acquisition from two representative specimens in the dataset. A typical room light image of each specimen is shown in the upper left-hand corner with regions of interest overlaid delineating tissue subtypes confirmed by histopathology. Raw, modulated images are shown on the left, and corresponding demodulated reflectance images are shown on the right. At the highest spatial frequency (f_x = 1.37 mm^{-1}), the demodulated reflectance contrast is dominated by scattering.

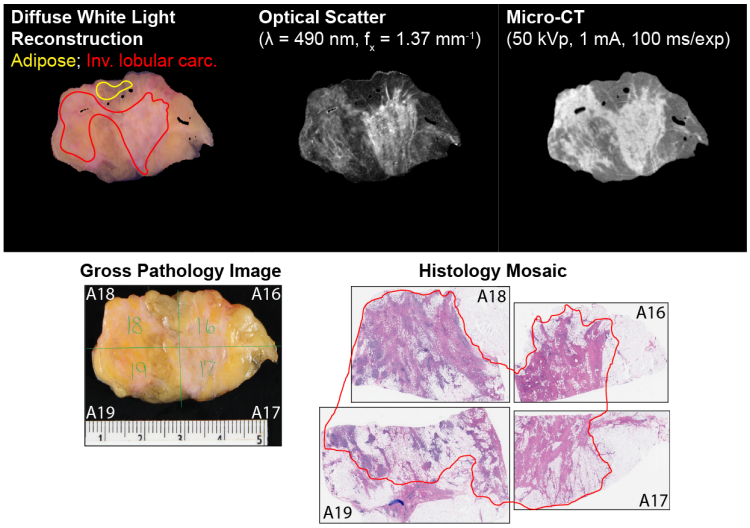

Figure S1. Demonstration of optical and micro-CT slice images co-registered with histopathology. ILCa = invasive lobular carcinoma; Ca = carcinoma; LCIS = lobular carcinoma *in situ.*

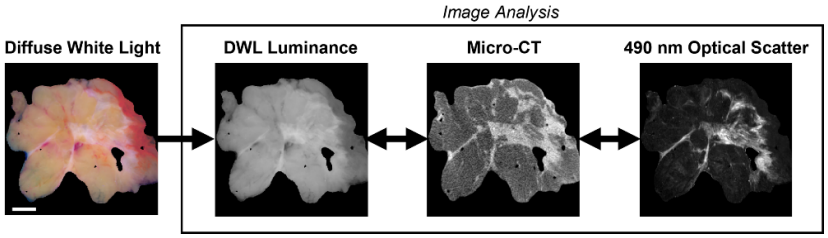

Figure S2. Similarity image analysis was performed on two pairs of grayscale image types: Room light luminance versus micro-CT and optical scatter versus micro-CT.

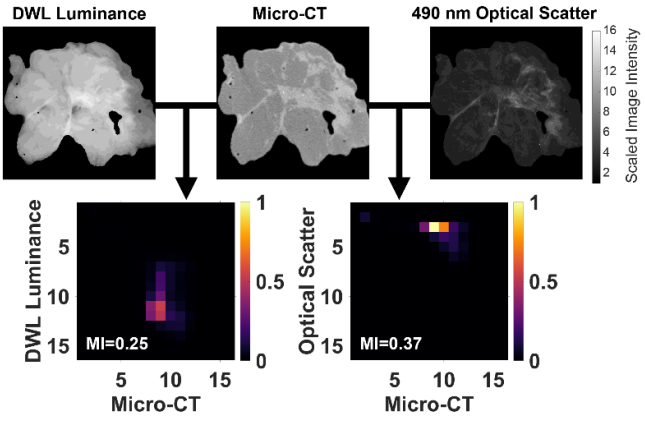

Figure S3. Mutual information was quantified using four-bit intensity scaled images (top row) and based on the joint histogram between each image type pair (bottom row). Joint histogram bin counts are normalized to the maximum optical scatter/micro-CT bin count value to emphasize the increased image similarity in the optical scatter/micro-CT image pair.

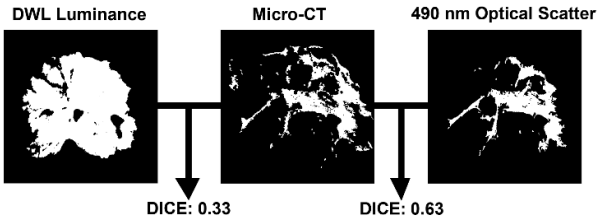

Figure S4. The Sørensen–Dice coefficient for each image pair was quantified from binarized versions of each image.

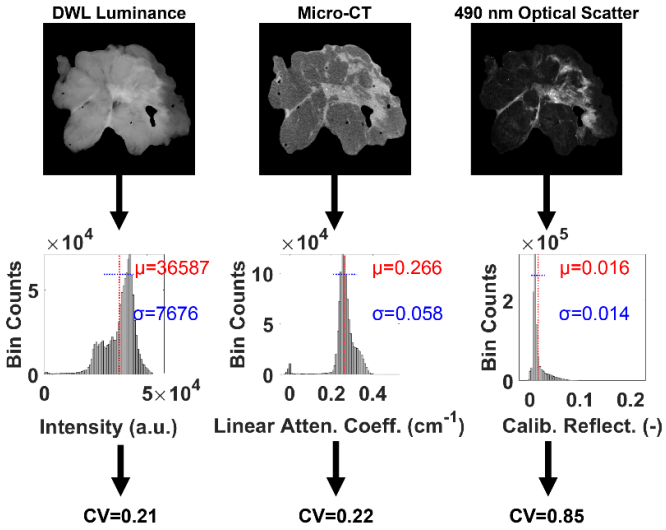

Figure S5. The coefficient of variation was defined as the standard deviation of pixel values (σ, blue horizontal lines in histograms) divided by the mean pixel value (μ, red vertical lines in histograms).